FA10 9:50

Proceedings of the 34th
Conference on Decision & Control
New Orleans, LA - December 1995

Control of Rotating Stall in a Low-Speed Axial Flow Compressor Using Pulsed Air Injection: Modeling, Simulations, and Experimental Validation

Robert L. Behnken*§
behnken@indra.caltech.edu

Raffaello D'Andrea†§
raff@hot.caltech.edu

Richard M. Murray‡§
murray@indra.caltech.edu

Division of Engineering and Applied Science
California Institute of Technology
Pasadena, California 91125

Abstract

Previous results in the use of pulsed air injection for active control of rotating stall have suggested that air injectors have the effect of shifting the steady state compressor characteristic. In this paper we analyze the effect of a compressor characteristic actuation scheme for the three state Moore Greitzer compression system model. It is shown that closed loop feedback based on the square magnitude of the first rotating stall mode can be used to decrease the hysteresis region associated with the transition from unstalled to stalled and back to unstalled operation. The compressor characteristic shifting idea is then applied to a higher fidelity distributed model in which the characteristic shifting has phase content in addition to the magnitude content captured by the three state model. The optimal phasing of the air injection relative to the sensed position of the stall cell is determined via simulation and the results found to agree with those obtained via an experimental parametric study on the Caltech low-speed axial flow compressor.

1. Introduction

As gas turbine engines have become better understood and better designed, increasing performance has begun to press the limits of what can be achieved without some type of control. Current state of the art is the use of open loop scheduling systems, where engine parameters are varied quasi-statically as the engine transitions between operating regions. The desire for still higher performance and greater efficiency, as well as improved sensing, actuation, and computation, have driven research into active control techniques.

Two of the limiting factors in the performance of compression systems are rotating stall and surge. Rotating stall refers to a dynamic instability that occurs when a nonaxisymmetric flow pattern develops in the blade passages of a compressor stage and forces a drastic reduction in the performance of the compressor. This degradation in performance is usually unacceptable and must be avoided. Surge is a large amplitude, axisymmetric oscillation in the compressor which results from exciting unstable dynamics in the overall pumping system. While surge and stall are separate phenomenon, the presence of stall is a precursor to the onset of surge in many compressor systems.

There are several active control techniques that have been shown to decrease the detrimental effects of rotating stall in axial flow compressors, including inlet guide vanes [13], bleed valves [1], and air injection [3]. In this work we concentrate on the use of pulsed on/off air injectors. The question is: can a set of air injectors placed in the upstream flow field change the compressor behavior with respect to rotating stall? A theoretical study of different actuation techniques performed in [5] suggested air injection to be one of the more promising choices for attenuation of rotating stall.

Ongoing work at Caltech is investigating the use of air injection for nonlinear control of rotating stall and surge in axial flow compressors. The eventual goal is to synthesize practical, nonlinear controllers for active control of propulsion systems. This includes not only the basic stability issues in axial flow compressors, but also disturbance rejection and transient performance problems. The Caltech compressor system consists of a nozzle, inlet duct, sensor and actuator ring, a single stage compressor without inlet guide vanes, an exit duct, and a throttle. Some previous work characterizing the effects of these ideas for open loop operation of these systems is presented in [6], [4], and [1]. Initial work towards active control using air injection is presented in [3] and [2], the latter includes a complete description of the low-speed axial compressor rig at Caltech which was used in the experimental results presented here.

In this paper we present an experimentally motivated model for air injector actuators which is based on the contrasts between the performance of the Caltech compressor for the unactuated and the fully actuated cases. In addition, we show that a simulation of this model captures some previously seen experimental results. The experimental work presented here differs from the results presented by Day in [3] in that the injectors are binary (on/off), not proportional, and in that the air injection is introduced at an angle relative to the mean flow through the compressor (see [2]). This non-zero air injection angle makes direct inclusion of these actuators in the Moore Greitzer model difficult.

The parametric study presented in [2] suggested that one possible method of modeling air injection was as an actuator for the steady state compressor characteristic; this was motivated by the drastic shift of the compressor performance curve between the case with no air injection and the case with continuous air injection as is shown in Figure 1. This shifting of the steady

*This material is based upon work partially supported under a NSF Graduate Research Fellowship.
†Author partially supported by NSERC.
‡Author partially supported by a grant from the Powel Foundation.
§Funding for this research was provided in part by AFOSR grant F49620-95-1-0409.

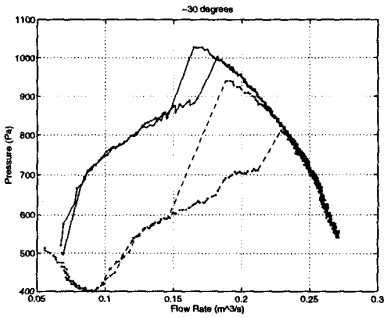

Fig. 1: Compressor characteristic for Caltech rig: performance without air injection (dashed line) vs. performance with continuous air injection (solid line).

state compressor characteristic curve can be used as a method of closed loop control since the unstalled region is extended when the air injection is on but at the cost of adding energy to the system. In this paper we explore the possibility of modeling the air injection as characteristic shifting for the three state Moore Greitzer model presented in [11] and the effects of this choice of feedback control law on the bifurcation diagram associated with these equations. This bifurcation analysis suggests which forms of shifting will change the hysteresis behavior of the closed loop system. We then search for a more local method of control using the shifting of the steady state compressor characteristic in simulations of the higher fidelity distributed model presented in [8] and compare the results to those obtained via a parametric study on the Caltech compressor. The results found experimentally for the optimal choice of phasing for pulsing of the air injectors relative to the position of the stall cell agree with the results obtained via simulation, suggesting that shifting of compressor characteristic is a good method for including the air injection actuators in this model.

2. Theory

2.1. Moore Greitzer three State Model

The results presented in this section are based on the model proposed by Moore and Greitzer in [11] with some changes in notation. The basic assumptions used to derive the equations used in this paper are presented here; for a complete derivation of the three state model (based on a single mode Galerkin projection) for a compression system see [11].

We begin with equations (44), (54), and (55) from [11] which are reproduced here for clarity:

$$\frac{d\psi}{d\xi} = \frac{1}{4l_cB^2}\left[\phi(\xi) - \gamma\sqrt{\psi}\right], \tag{1}$$

$$\frac{1}{2\pi}\int_0^{2\pi} \Psi_c(\phi + A\sin\zeta)d\zeta = \psi + l_c\frac{d\phi}{d\xi}, \tag{2}$$

and

$$\frac{1}{\pi}\int_0^{2\pi} \Psi_c(\phi + A\sin\zeta)\sin\zeta d\zeta = \left(m + \frac{1}{a}\right)\frac{dA}{d\xi} \tag{3}$$

where W in [11] has been set to 1, ψ is the average pressure rise coefficient, ϕ is the average flow coefficient, A is the amplitude of the sinusoidal flow coefficient perturbation, ξ is dimensionless time, Ψ_c is the steady state compressor characteristic, γ is the throttle position, and l_c, B, a, and m are parameters which depend on the compression system. Based on the experimental results described in [2] we attempt to model the air injection actuators as direct actuators of the steady state compressor characteristic. In this paper we analyze the results of the closed loop system where the feedback is proportional to the size of the first mode of the stall cell squared:

$$\Psi_c = \Psi + KA^2\overline{\Psi} \tag{4}$$

where

$$\Psi = a_0 + a_1\phi + a_2\phi^2 + a_3\phi^3 \qquad \overline{\Psi} = c_0 + c_1\phi. \tag{5}$$

By performing the integrals indicated above and substituting $J = A^2$, we obtain the following set of ODE's which describe the dynamics of the compression system;

$$\dot{\psi} = \alpha\left(\phi - \gamma\sqrt{\psi}\right), \tag{6}$$

$$\dot{\phi} = \beta\left(\Psi_c - \psi + \frac{J}{4}\frac{\partial^2\Psi_c}{\partial\phi^2}\right), \tag{7}$$

and

$$\dot{J} = \delta J\left(\frac{\partial\Psi_c}{\partial\phi} + \frac{J}{8}\frac{\partial^3\Psi_c}{\partial\phi^3}\right) \tag{8}$$

where

$$\alpha = \frac{1}{4l_cB^2} \qquad \beta = \frac{1}{l_c} \qquad \delta = \frac{2a}{1+ma}. \tag{9}$$

2.2. Bifurcation Analysis

The bifurcation properties of the open loop three state compression system model were initially studied by McCaughan in [9] and [10]. There the bifurcations for the pure rotating stall case, the pure surge case, and combination stall/surge case were thoughly investigated. A throttle based closed loop system for the pure rotating stall case was developed and analyzed by Liaw and Abed in [7].

In this paper we are interested only in the pure rotating stall case for the closed loop compression system with the control based on shifting of the steady state compressor characteristic. For the open loop case, the bifurcation diagram for a representative compressor characteristic is known to have a transcritical bifurcation (for the choice of coordinates used in this paper) at the point which corresponds to operating at the peak of the steady state compressor characteristic (see Figure 2). The throttle setting which corresponds to the peak of the characteristic, $(\partial\Psi_c/\partial\phi) = 0$, will be denoted by γ^*. This operating point corresponds to where the stalled branch intersects the horizontal axis in the bifurcation diagram shown in Figure 2.

The unstable sections of the bifurcation diagram in Figure 2 are shown as grey lines, and the stable sections are shown as black lines. This diagram suggests a hysteresis region since as the throttle is closed (γ is decreased) $J = 0$ is a stable solution until γ^* is reached, at which point the stable solution for J is non-zero (which corresponds to a jump to rotating stall). As γ continues to decrease, the stable solution for J continues to be non-zero. If the throttle is then opened, beginning at $\gamma < \gamma^*$, the system continues to evolve

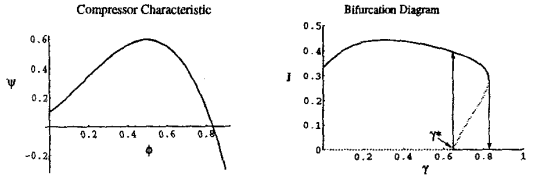

Fig. 2: Bifurcation diagram showing jumps associated with the hysteresis loop for an open loop compression system with the characteristic shown at the left (pure rotating stall case).

along the stalled branch until γ is increased to a value substantially greater than γ^* before returning to the $J = 0$ branch. The system has substantially different solutions depending on the path that γ follows. We next analyze how the closed loop system based on a shifting of the steady state compressor characteristic effects this bifurcation diagram and in particular the hysteresis region.

Here we present one method for changing the hysteresis behavior of the compression system by selecting a control input which directly changes the bifurcation diagram in the hysteresis region. A shifting of the steady state compressor characteristic curve proportional to J, as suggested earlier, can accomplish this. To see how, we first solve for the slope of the bifurcation curve at the point γ^*. On the stalled branch of the bifurcation diagram, the following algebraic equations must hold

$$\phi^2 = \gamma^2 \psi, \tag{10}$$

$$\Psi_c = \psi - \frac{J}{4}\frac{\partial^2 \Psi_c}{\partial \phi^2}, \tag{11}$$

and

$$\frac{\partial \Psi_c}{\partial \phi} = -\frac{J}{8}\frac{\partial^3 \Psi_c}{\partial \phi^3}. \tag{12}$$

Noting that, for each equilibrium solution on the stalled branch of the bifurcation diagram, choosing J fixes ϕ, ψ, and γ, and by differentiating equation (10) with respect to J we obtain

$$2\phi\frac{d\phi}{dJ} = 2\gamma\frac{d\gamma}{dJ} + \gamma^2\frac{d\psi}{dJ}. \tag{13}$$

By differentiating equation (11) with respect to J, an expression for $\frac{d\psi}{dJ}$ at the peak of the compressor characteristic is found to be

$$\left.\frac{d\psi}{dJ}\right|_{\gamma=\gamma^*} = K\overline{\Psi} + \frac{1}{4}\frac{\partial^2 \Psi}{\partial \phi^2}. \tag{14}$$

By similar differentiation of equation (12) with respect to J, an expression for $(d\phi/dJ)$ at the same point is found to be

$$\left.\frac{d\phi}{dJ}\right|_{\gamma=\gamma^*} = \frac{K\frac{\partial \overline{\Psi}}{\partial \phi} + \frac{1}{8}\frac{\partial^3 \Psi}{\partial \phi^3}}{-\frac{\partial^2 \Psi}{\partial \phi^2}}. \tag{15}$$

If equations (14) and (15) are substituted into equation (13) and the result solved for $(dJ/d\gamma)$, the slope of the bifurcation diagram at the equilibrium point associated with γ^* is obtained as:

$$\left.\frac{dJ}{d\gamma}\right|_{\gamma=\gamma^*} = \frac{\sqrt{\psi}}{\frac{K\overline{\Psi}_\phi + \frac{1}{8}\Psi_{\phi\phi\phi}}{-\Psi_{\phi\phi}} - \frac{\phi}{2\psi}\left(K\overline{\Psi} + \frac{1}{4}\Psi_{\phi\phi}\right)}, \tag{16}$$

where all expressions in the right hand side of equation (16) are evaluated at the equilibrium point at the peak of the compressor characteristic, and the subscript ϕ denotes partial differentiation.

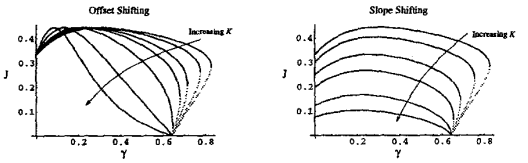

Fig. 3: Change in bifurcation diagram as K is varied: $c_0 = 1$, $c_1 = 0$ and $c_0 = 0.5$, $c_1 = -1$.

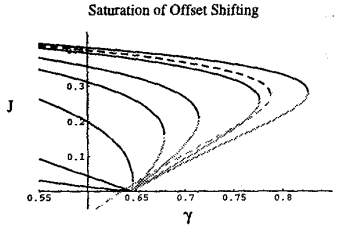

Fig. 4: Bifurcation diagram showing 20% saturation limits (dashed line) for offset shifting.

From this expression it is easy to see how varying the gain on the shifted characteristic affects the slope of the bifurcation diagram at γ^*. Typically, $(dJ/d\gamma)|_{\gamma=\gamma^*}$ is positive (as is shown in the bifurcation diagram in Figure 2) and if this positive value were increased, the size of the hysteresis region could be decreased. If the shifted portion of the characteristic, $\overline{\Psi}$, has a positive offset term ($c_0 > 0$) the slope will be increased by a positive gain K, and if the shifted characteristic has a negative linear term ($c_1 < 0$) the slope will also be increased for a positive gain K.

Figure 3 shows how the bifurcation diagram changes as the gain K is increased for a pure offset shift at the peak of the compressor characteristic (left) and for a pure slope shift (right) for the compressor characteristic shown at the left of Figure 2.

This same sort of analysis can also be used to show how the hysteresis loop in the bifurcation diagram cannot be changed with nonlinear feedback of ψ or ϕ via throttle control (as was previously shown in [7]).

2.3. Effects of Saturation

The entire family of bifurcation diagrams shown in Figure 3 may not be physically possible in practice; there will be a maximum amount that the steady state compressor characteristic can be shifted. Figure 1 shows the maximal amount that that the characteristic can be shifted for the actuators installed on the Caltech compressor. This saturation of the actuators translates to direct limit on how much the closed loop bifurcation diagram can be modified. In Figure 4 the dashed line shows the saturation limit for 20% shift in the offset term of the characteristic perturbation, c_0, from the base value of a_0. Shifts which lie to the right of the saturation line are allowed, and for shifts which lie to the left, the saturation line becomes the curve that describes the system behavior.

Based on the previous analysis, the amount of characteristic shifting required to eliminate the rotating stall hysteresis loop would be the amount which equation (16) is infinite. In practice this calculation is very

conservative. In most applications, noise will drive the compressor into rotating stall at a value of γ which is substantially greater than γ^*. This throttle position will therefore dictate the amount that the characteristic must be shifted to eliminate the hysteresis loop.

3. Simulation

The motivation for introducing a steady state compressor characteristic which varies based on a control input was the modeling of the air injectors used on the Caltech compressor. In this section we attempt to use the insights gained from the analysis on the three state model on a higher fidelity model. The model used here is the distributed model presented in [8], which is basically a system of equations describing the dynamics of the flow coefficient ϕ at discrete points around the compressor annulus. The model is attractive because the steady state compressor characteristic shifting can be included in local way instead of as an average shift as was done in the previous analysis. The compressor characteristic can then be shifted in phase as well as in magnitude. The distributed model was used to search for the optimal phasing of the compressor characteristic shifting. We first present the equations of the basic distributed model and then describe the search for the optimal phasing via simulation.

3.1. Local Compressor Characteristic Shifting

The full details of the distributed model presented in [8] should be obtained from that reference; only the details required to explain how the compressor characteristic shifting was included in the model will be presented here. The final equations (equation (20)) from [8] which make up the distributed model for a compression system are given by:

$$\dot{\bar{\psi}} = \frac{1}{4l_c B^2}\left(S\phi - \gamma\sqrt{\bar{\psi}}\right) \tag{17}$$

and

$$G^{-1}D_E G\dot{\phi} = -G^{-1}D_A G\phi + \Psi_c(\phi) - T\bar{\psi}, \tag{18}$$

where $\bar{\psi}$ is the annulus averaged pressure rise coefficient, ϕ is the vector of flow coefficients at discrete points around the compressor annulus, γ is the throttle position, D_A, D_E, T, S, B and l_c are constants which depend on the compressor rig (see [8]), and G is the discrete Fourier transform matrix, i.e.

$$\phi = \begin{bmatrix} \phi_1 \\ \phi_2 \\ \vdots \\ \phi_{2n+1} \end{bmatrix} \qquad G : \phi \mapsto \begin{bmatrix} \bar{\phi}_0 \\ \mathrm{Re}\,\bar{\phi}_1 \\ \mathrm{Im}\,\bar{\phi}_1 \\ \vdots \\ \mathrm{Re}\,\bar{\phi}_n \\ \mathrm{Im}\,\bar{\phi}_n \end{bmatrix}$$

where $\bar{\phi}_i$ is the Fourier coefficient associated with mode i and n is the number of modes included in the model.

The Caltech compressor rig has three air injectors placed 120 degrees apart around the compressor annulus, and each injector has an affect on a small region of the compressor rotor. In the distributed model, the vector of pressure rise coefficients around the compressor annulus is given by Ψ_c. In order to include the compressor characteristic shifting as a local effect, the shift is included as:

$$\Psi_c(\phi_i) = \Psi(\phi_i) + KJ(c_0 + c_1\phi_i) \tag{19}$$

at the three points around the annulus which have injectors associated with them (for 4 modes, $i = 1, 4, 7$) and as

$$\Psi_c(\phi_i) = \Psi(\phi_i) \tag{20}$$

for the remaining positions (for 4 modes, $i = 2, 3, 5, 6, 8, 9$). As with the three state model, a cubic in ϕ is used for the nominal value of the steady state compressor characteristic,

$$\Psi(\phi_i) = a_0 + a_1\phi_i + a_2\phi_i^2 + a_3\phi_i^3. \tag{21}$$

3.2. Simulation Study

A simulation study was performed to find the optimal phase window (phasing) for a rotating stall controller using the shifting compressor characteristic to model the air injectors. The phase window of an injector refers to a particular sector of the compressor annulus. During the study, an injector was turned on if the stall cell was located within that injector's phase window, and the parametric study consisted of gridding the space of phase windows and simulating all cases. The model used was that of the MIT c2 compressor rig described in [8], with the compressor characteristic shifting implemented as described above.

In the simulations the compressor characteristic associated with a each injector was shifted when the stall cell's measured location was within that injector's 120 degree wide phase window. For the first case, the position of the center of the first injector's window was fixed at zero degrees, and the positions of the windows for the other two injectors were varied. With the phasing of the first injector fixed, the center position of the second injector's window was set to zero degrees, and twelve tests were performed as the window position of the third was varied from zero to 330 degrees in steps of 30 degrees. With the first window still fixed, the second window was increased to 30 degrees, and the third window was again cycled from zero to 330. This test was repeated as the second window was cycled up to 330 degrees, resulting in 144 different controllers tested for the first window fixed at zero degrees.

The second test was the same except that the first window was incremented to 30 degrees. Twelve choices for the phasing of the first injector brought the total number of controllers tested to 1728.

For each controller tested the average amplitude of the first mode stall cell was recorded. The results for the phasing of injector one (and all choices of phasing for injectors two three) which produced the broadest band of minima is shown at the top of Figure 5. The result shown is for a window around injector one centered at zero degrees. The second plot shows the choice of phasing for the second injector (for the 144 tested phasing combinations of injectors one and three) and corresponds to a window centered at 120 degrees. The final plot shows the results for injector three, and corresponds to a window centered at 240 degrees. In each plot, the optimal phasing is shown as a solid line, a non-optimal phasing is shown as a dotted line, and a * marks the optimal controller in each plot.

In all the simulations presented here, the same initial stall cell disturbance (both in magnitude and phase) was used. It should be noted that this and the nonlinear growth rate of the stall cell cause any symmetries in the three plots of Figure 5 to break down, i.e. we would

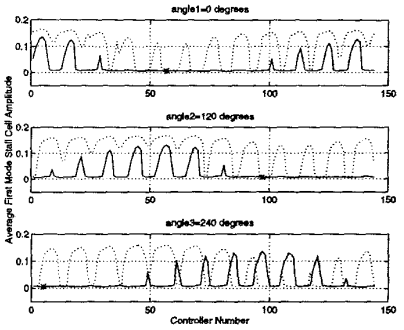

Fig. 5: Simulation parametric study results: average amplitude of first stall mode vs. controller number, see text for complete discription.

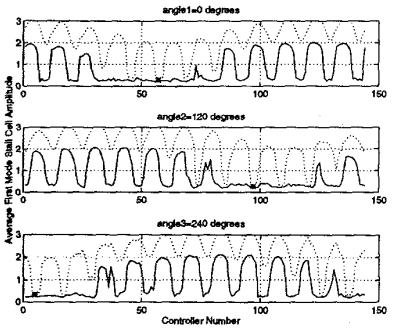

Fig. 6: Experimental parametric study results: average amplitude of first stall mode vs. controller number, see text for complete discription.

not expect the three plots to be be shifted versions of one another because while the geometry of the system is symmetric, the initial conditions are not.

4. Experimental Verification

Previous work on using pulsed air injectors to control rotating stall was presented in [2]; initial work towards locating an optimal controller was presented there as well as a complete description of the Caltech compression system. A short summary of that work is presented here in order to present further experimental results supporting the distributed model simulations.

The Caltech compressor is an axial flow compressor driven by an electric motor. The rig is instrumented with pressure transducers slightly upstream of the rotor which are used to determine the amplitude and phase of the first and second modes of rotating stall. Additional pressure sensors are used to determine the pressure rise and flow rate at any given time. A PC based data acquisition system running the Sparrow real-time control kernel [12] was used for the experiments presented here. The rig was operated at a rotor frequency of 100 Hz which corresponds to a mass flow of 0.19 m^3/sec and a pressure rise of 940 Pa at the peak of the steady state compressor characteristic (see Figure 1). The frequency of the first mode of rotating stall for this rig under these operating conditions is 64.5 Hz. Three air injectors placed 120 degrees apart around the compressor annulus just upstream of the rotor were used as actuators, and these injectors had a maximal control authority (in terms of energy) of two percent relative to the total work produced by the compressor. For further information about the system see [2].

4.1. Parametric Study

A parametric study was performed on the Caltech compressor to determine the optimal phasing for turning the air injection actuators on relative to the measured position of the first mode stall cell. In the study, the amount of time that the injector was left on after the initial instruction to turn on was fixed at 7.5 msec. After the delay time for the opening of the injector is taken into account, this corresponds to roughly one third of the time required for the stall cell to make a complete revolution around the compressor annulus.

In the experimental study, the compressor was operated near enough to the peak of the steady state compressor characteristic that the system would spontaneously go into rotating stall when no control action was used. For the first test, the phase between the sensed position of the stall cell and when the first injector was opened was fixed at zero, i.e. the injector was instructed to open exactly when the stall cell passed it. With the phase of the first injector fixed, the phase of the second and third injectors were varied from zero to 330 degrees in 30 degree intervals (so 144 different phasings were tested for the phasing of injector one fixed at zero degrees). The phasing of injector one was then increased to 30 degrees and 144 additional controllers were tested as the phasing of injectors two and three were varied as in the first test. These tests were performed for the phasing of injector one fixed at values from zero to 330 degrees in 30 degree intervals, bringing the total number of controllers tested to 12*144=1728.

For each of the 1728 controllers tested, the average size of the stall cell while the controller was on was recorded. One criteria for the best controller is then the controller that had the lowest value for the average stall cell size. Other criteria were also investigated (total time that injectors were on for example) and all produced roughly the same results. Figure 6 shows the results for the optimal choice of phasing for each of the three air injectors. The top plot in Figure 6 shows the average stall cell size versus the controller number (1-144) for the center of the phase window of injector one fixed at zero degrees; each controller number corresponds to a different choice of phasing for injectors two and three. The choice of zero degrees is optimal with respect to other choices for the phasing of injector one because it allows for the largest uncertainty in the choice of phasings of the other injectors. The lower two plots show the optimal phasing choices for injectors two and three. In each plot, the controller with optimal phasing is shown as a solid line, a controller with non-optimal phasing is shown as a dotted line, and a * marks the optimal controller in each plot.

The experimentally determined optimal controller can be easily visualized as is shown in Figure 7. In the figure, the light region corresponds to an area of higher pressure (stalled region), the boxes represent the position of the injector which is open, and the stall cell is rotating counter-clockwise. The stall cell position relative to the actuator when the injector opens is shown on the left and the stall cell position at the last instant

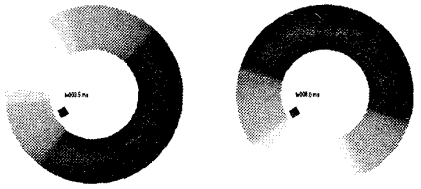

Fig. 7: Visualization of optimal controller found via experimental search.

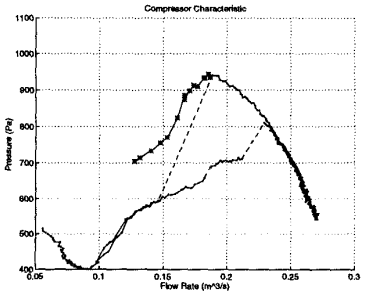

Fig. 8: Closed loop compressor characteristic for the optimal controller, no hysteresis.

that the injector is open is shown on the right. More intuitively, the controller attempts to increase the flow in the regions of the rotor that are stalled.

The closed loop compressor performance curve is shown in Figure 8 for an optimal choice of injector phasings. The results shown to the left of the peak of the characteristic are time averaged values, since in this region the system is constantly rejecting the formation of stall. This figure shows that the air injection controller has eliminated the hysteresis region associated with the transition into and out of stall.

4.2. Comparisons with Simulation

The optimal phasing for injectors determined via experimentation is qualitatively very similar to the result obtained with the compressor characteristic shifting model for the air injectors. The simulation study shows the same sensitivity to the phasing of a single injector when the phase of the other two injectors is held constant. This is shown by the twelve individual local minima that occur the plots obtained via simulation shown in Figure 5 and those from the experiment shown in Figure 6.

The strongest similarity is that the simulation and the experimental results both show that the optimal controller has the three injectors turning on exactly 120 degrees out of phase and furthermore, that the air injection should not lead or lag the stall cell position.

5. Conclusions and Future Work

In this paper we have analyzed the effects of a shifting of the steady state compressor characteristic on the transcritical bifurcation associated with pure rotating stall for the three state Moore Greitzer compressor model. We have also shown the form of the compressor characteristic shifting required to change the size of the hysteresis loop associated with rotating stall. The family of bifurcation diagrams associated with a feedback controller based on these forms of characteristic shifting have been presented for a specific example. The effects of saturation have been described based on the bifurcation diagram for the closed loop system.

Using the ideas gained from analyzing annulus averaged compressor characteristic shifting on the three state model, we have extended a higher fidelity compression system model (one which captures more of the local behavior of these systems) to include a closed loop controller based on local characteristic shifting. Parametric studies were performed using simulations and using the Caltech compressor, both of which produced qualitatively very similar results for the optimal controller. Finally, the experimental controller showed complete elimination of the hysteresis region associated with the transition into and out of rotating stall.

Future work will involve predicting the quantitative results of the closed loop compression system (including the closed loop compressor characteristic) via simulations. To this end, we are currently developing higher fidelity models for the Caltech compressor rig. Including surge dynamics into the analysis, simulations, and experiments as well as throttle based control techniques are also part of our on-going work. The final goal is full control of rotating stall and surge using a combination of air injectors and throttle controllers.

References

[1] O. O. Badmus, S. Chowdhury, K. M. Eveker, and C. N. Nett. Control-oriented high-frequency turbomachinery modeling - single-stage compression system one-dimensional model. *Journal of Turbomachinery*, 117:47–61, January 1995.

[2] R. D'Andrea, R. L. Behnken, and R. M. Murray. Active control of rotating stall using pulsed air injection: A parametric study on a low-speed, axial flow compressor. In *Sensing, Actuation, and Control in Aeropropulsion; SPIE International Symposium on Aerospace/Defense Sensing and Dual-Use Photonics*, pages 152–165, 1995.

[3] I. J. Day. Active supression of rotating stall and surge in axial compressors. *Journal of Turbomachinery*, 115:40–47, 1993.

[4] I. J. Day. Stall inception in axial flow compressors. *Journal of Turbomachinery*, 115:1–9, 1993.

[5] G. J. Hendricks and D. L. Gysling. Theoretical study of sensor-actuator schemes for rotating stall control. *Journal of Propulsion and Power*, 10(1):101–109, 1994.

[6] A. Khalak and R. M. Murray. Experimental evaluation of air injection for actuation of rotating stall in a low speed, axial fan. In *Proc. ASME Turbo Expo*, 1995.

[7] D. C. Liaw and E. H. Abed. Active control of compressor stall inception: A bifurcation-theoretic approach. Technical report, Institute for Systems Research, Univ. of Maryland, 1992. Also appears in Proceedings of NOLCOS '92 , M. Fliess, ed., Pergammon Press.

[8] C. A. Mansoux, D. L. Gysling, J. D. Setiawan, and J. D. Paduano. Distributed nonlinear modeling and stability analysis of axial compressor stall and surge. In *Proc. American Control Conference*, pages 2305–2316, 1994.

[9] F. E. McCaughan. Application of bifurcation theory to axial flow compressor instability. *Journal of Turbomachinery*, 111:426–433, 1989.

[10] F. E. McCaughan. Bifurcation analysis of axial flow compressor stability. *SIAM Journal of Applied Mathematics*, 20(5):1232–1253, 1990.

[11] F. K. Moore and E. M. Greitzer. A theory of post-stall transients in axial compression systems—Part I: Development of equations. *Journal of Turbomachinery*, 108:68–76, 1986.

[12] R. M. Murray and E. L. Wemhoff. *Sparrow 2.0 Reference Manual*. California Institute of Technology, 1994.

[13] J. D. Paduano, A. H. Epstein, L. Valavani, J. P. Longley, E. M. Greitzer, and G. R. Guenette. Active control of rotating stall in a low-speed axial compressor. *Journal of Turbomachinery*, 115:48–56, January 1993.